JETIR.ORG ISSN: 2349-5162 | ESTD Year : 2014 | Monthly Issue
JOURNAL OF EMERGING TECHNOLOGIES AND INNOVATIVE RESEARCH (JETIR)
An International Scholarly Open Access, Peer-reviewed, Refereed Journal

Finite Element Analysis of convective Heat Transfer flow of Ethylene Glycol based SWCNT and MWCNT Rotating Nanofluids in a Vertical Channel with Variable Viscosity, Activation energy, Heat Generating Sources and Hall Effects

Srijana Sharma[1] and Prof. D.R.V. Prasada Rao[2]
[1]P.G. Mathematics Student, Mobile : +91 6000377701, Email- srijanakoushik@gmail.com
[2]Distinguish Visiting Faculty of Mathematics, Central University of Andhra Pradesh Transit Campus–II, CRIT Campus,Ananthapuramu-505001,Andhra Pradesh,

Abstract **:**An attempt has been made to analyse the combined effect of variable viscosity, activation energy, thermal radiation on convective heat and mass transfer flow of Ethylene glycol based Swcnt and Mwcnt nanofluids through porous medium in a vertical channel in the presence of heat generating sources. The governing equations of the flow, heat and mass transfer of nanofluids have been executed by Finite element technique.The velocity, temperature and nanoconcentration have been analysed for different parametric variations through graphs. The skin friction, rate of heat and mass transfer on the channel walls are numerically evaluated. The observation of the velocities depreciate, temperature enhances with increase in G/Ec. Increase in Hall parameter(m)/ viscosity parameter(B)/ radiation(Rd) enhances u, w, θ. Velocity, temperature reduce, transverse velocity(w) enhances with higher values of rotation parameter (R)/ heat source parameter(Q)/nanoparticle volume fraction(φ). The nanoconcentration(C) decays with increase in activation energy(E1)/Soret parameter(Sr).

Keywords : Egbased Swcnt and Mwcnt nanofluids,Vertical channel,activation energy, Soret effect, Hall effect, Rotation, Thermal radiation,Heat sources.

1. INTRODUCTION:

The carbon nanotubes (CNT's) have become one of the most effective materials, owing to their ability to enhance the thermal characteristics of the fluid, high electrical conductivity, unique optical transmission, and high tensile strength. They can also increase the entropy generation Berrehal [4]. Shafiq et al [13] CNT'S are rolled–up graphene sheets arranged in a cylindrical shape. They are of two types single walled (SWCNT's)) and multi-walled (MWCNT's). It was observed that the boundary layer separation could be delayed if suction effects on the CNT's nanoparticle volume fraction are provided Anuar [1]. Naganthran et al [11], CNT's have higher thermal conductivity. Shamshuddin et al [14] have studied the dynamics of ethylene glycol conveying Mwcnts and Ethylene glycol conveying Swcnts: Significant joule heating and thermal radiation. Vijayalakshmi [20] has explored the effect of thermal radiation on non-Darcy hydromagnetic convective heat and mass transfer flow of a water-Swcnt's nanofluid in a cylindrical annulus with thermo-diffusion and chemical reaction. Several authors (Shamshuddin et al[15], Srinivasa Rao and Shamshuddin [17]) have examined the influence of heat sources on Conceptive heat transfer flow.

The vertical channel is an often encountered configuration in thermal engineering equipment, as an example, collectors of solar power, cooling devices of digital and micro-digital equipments and many others. The radiation effect on a hydromagnetic convective flow in a vertical channel was studied by Gupta and Gupta [8]. Datta and Jana [5] have studied the effect of wall conductance on a hydromagnetic convection of a radiation gas in a vertical channel. The combined forced and free convective flow in a vertical channel with viscous dissipation and isothermal–isoflux boundary conditions have been studied by Barletta [3].

Sulochana and Ramakrishna [18] have analyse effect of dissipation, thermal radiation, radiation absorbtion on convective heat and mass transfer flow in a non-uniformly heated vertical channel. Arundhati et el [2] have discussed thermal radiation and thermo-diffusion effect on convective heat and mass transfer flow of a rotating nanofluid in a vertical channel. Sreedevi et al [16] & Kiran Kumar et al [9] have analyse effect of dissipation and radiation on convective heat transfer flow of a rotating cu-water nano-fluid in a vertical channel.

The model with potential reactants to produce a chemical reaction minimizing the energy in the chemical system is focused nowadays in the industrial manufacturing of extrusion of plastic, aerodynamics with rubber sheets crystal growing, geothermal or oil reservoir engineering and so on (Dhlamini et al. [6]). The Arrhenius activation terminology was first indicated by Svante Arrhenius around 1889. One significant measure in free convection boundary layer flows taking into account heat mass transfer together is the specific chemical reactions with finite Arrhenius activation energy. It is more significant to put on the theoretical attempts to predict the advantages of the activation energy inflows mentioned above instead of the experimental works

in these areas (Maleque [10], Netai and Dulal [12]). Suvarna [19] has discussed finite element approach of hydromagnetic heat and mass transfer flow of rotating fluid in a channel with activation energy. Recently Gopi [7] has extended this work to include theeffect of heat generating sources on hydromagnetic convective heat transfer flow of rotating Swcnt and Mwcnt nanofluids in a vertical channel with inconstant viscosity.

In this paper we investigate the combined influence of variable viscosity, activation energy, thermal radiation on convective heat and mass transfer flow of Ethylene glycol based Swcnt and Mwcnt nanofluids through porous medium in a vertical channel in the presence of heat generating sources. The non-linear,coupled equations governing the flow, heat and mass transfer of nanofluids have been solved by Finite element technique with quadratic interpolation functions. The behaviour of the velocity, temperature and concentration have been discussed for different parametric variations. The skin friction, rate of heat and mass transfer on the channel walls are numerically evaluated for different variations.

2. FORMULATION OF THE PROBLEM:

We consider the steady, threedimensional flow of a nanofluid consisting of a Ethylene glycol based Swcnt and Mwcnt nanofluids in a vertical porous channel with thermal radiation. A uniform magnetic field of strength Ho is applied normal to the plate. It is assumed that there is no applied voltage which implies the absence of an electric field. The flow is assumed to be in the x-direction which is taken along the plane in an upward direction and z-axis is normal to the plate. It is assumed that the whole system is rotating with a constant angular velocity vector $\overline{\Omega}$ about the y-axis. The fluid is assumed to be gray, absorbing,emitting but not scattering medium. The radiation heat flux in the x-direction is considered negligible in comparison with that in the y-direction. Due to the fully developed assumption, the flow variables are functions of y only. Figure.1 shows that the problem under consideration and the co-ordinate system.

In the present problem, the following assumptions have been made: The conservation equation of current density $\nabla.\bar{J} = 0$ gives Jy=constant.

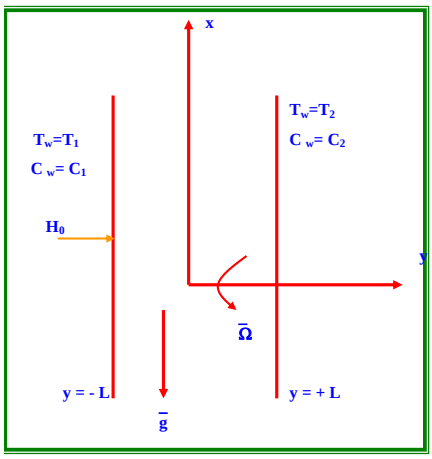

Figure 1 . Schematic diagram of the problem

Under the abovementioned assumptions, the equation of momentum and thermal energy respectively under Rosseland approximation can be written in dimensional form as:

$$\frac{\partial u}{\partial x}+\frac{\partial v}{\partial y}=0 \tag{2.1}$$

$$\rho_{nf}(v\frac{\partial u}{\partial y}-2\Omega w)=\frac{\partial}{\partial y}(\mu_{nf}(T)\frac{\partial u}{\partial y})+(\rho_f\beta_T)_{nf}\,g(T-T_2)-(\frac{\mu_{nf}}{k_p})u-\frac{\sigma_{nf}B_o^2}{(1+m^2)}(u+mw) \tag{2.2}$$

$$\rho_{nf}(v\frac{\partial w}{\partial y}+2\Omega u)=\frac{\partial}{\partial y}(\mu_{nf}(T)\frac{\partial w}{\partial y})-(\frac{\mu_{nf}}{k_p})w+\frac{\sigma_{nf}B_o^2}{(1+m^2)}(mu-w) \tag{2.3}$$

$$(\rho C_p)_{nf}(v\frac{\partial T}{\partial y})=k_{nf}\frac{\partial^2 T}{\partial y^2}-\frac{\partial(q_R)}{\partial y}+Q_H(T-T_2)+$$
$$+2\mu_{nf}[(\frac{\partial u}{\partial y})^2+(\frac{\partial w}{\partial y})^2]+\frac{\sigma_{nf}\mu_e^2H_o^2}{1+m^2}(u^2+w^2) \tag{2.4}$$

$$u\frac{\partial C}{\partial y}=D_B\frac{\partial^2 C}{\partial y^2}+\frac{D_T}{T_m}(\frac{\partial^2 T}{\partial y^2})-kc(C-C_2)(\frac{T}{T_2})^n Exp(-\frac{E_a}{KT}) \tag{2.5}$$

The boundary conditions are:

$$\begin{aligned} &u(\pm L)=0 \quad , \quad && w(\pm L)=0, \\ &T(-L)=T_1 \ , && T(+L)=T_2 \\ &C'(-L)=C_1 \ , && C'(+L)=C_2 \end{aligned} \tag{2.6}$$

The properties of the nanofluids are defined as follows:

$$\mu_{nf} = \mu_f/(1-\varphi)^{2.5} \qquad \alpha_{nf} = \frac{k_{nf}}{(\rho C_p)_{nf}} \qquad \rho_{nf} = (1-\varphi)\rho_f + \varphi\rho_s$$
$$(\rho C_p)_{nf} = (1-\varphi)(\rho C_P)_f + \varphi(\rho C_P)_s \qquad (\rho\beta)_{nf} = (1-\varphi)(\rho\beta)_f + \varphi(\rho\beta)_s$$
$$k_{nf} = \frac{k_f(k_s+2k_f-2\varphi(k_f-k_s)}{(k_s+2k_f+2\varphi(k_f-k_s)}, \sigma_{nf} = (\sigma_f + \frac{3(\sigma_f-\sigma_s)\phi}{(\sigma_s+2\sigma_f)}), \quad (2.7)$$

where the subscripts nf, f and s represent the thermophysical properties of the nanofluid, base fluid and the nanosolid particles respectively and ϕ is the solid volume fraction of the nanoparticles. The thermophysical properties of the nanofluid are given in Table 1.

Table – 1 : Physical Properties of nanofluids

Physical properties	Fluid phase (Ethylene Glycol)	**Swcnt**	**Mwcn**
C_p(j/kg K)	**2430**	**425**	**796**
ρ(kg m^3)	**1115**	**2600**	**1600**
k(W/m K)	**0.253**	**6600**	**3000**
βx10^{-5} 1/k)	5.7	27	**44**
σ	**10.7**	**1**	**1**

We consider the solution of equation(2.1) as:

$v=-v_0$ (2.8)

The dynamic viscosity of the nanofluids is assumed to be temperature dependent as follows:

$$\mu_{nf}(T) = \mu_f Exp(-m(T-T_2)) \quad (2.9)$$

where μ_{nf} is the nanofluid viscosity at the ambient temperature To, m is the viscosity variation parameter which depends on the particular fluid.

We introduce the following dimensionless variables:

$$y' = \frac{y}{L}, u' = \frac{u}{v_0}, w' = \frac{v}{v_0}, \theta = \frac{T-T_2}{T_1-T_2}, C = \frac{C'-C_2}{C_1-C_2}, G = \frac{\beta g(T_1-T_2)L^2}{\mu_f v_o}, B = m(T_1-T_2),$$
$$S = \frac{v_0 L}{\mu_f}, \ M = \frac{\sigma_f \mu_e^2 H_0^2 L^2}{\rho_f \mu_f}, \ Q = \frac{Q_H L^2}{k_f}, \ Rd = \frac{4\sigma^{\bullet} T_0^3}{\beta_R k_f}, So = \frac{D_B K_T (C_1-C_2)}{T_m (T_1-T_2)}, \gamma = \frac{k_c L^2}{D_B} \quad (2.10)$$

Equations(2.2)-(2.4) in the non-dimensional form under Rosseland approximation are

$$0 = (\frac{\partial^2 u}{\partial y^2} - B\frac{\partial u}{\partial y}\frac{\partial \theta}{\partial y}) + Exp(B\theta)[A_1A_3(-S\frac{\partial u}{\partial z} + 2Rw) + + A_1A_4G(\theta) - A_1A_6\frac{M^2}{1+m^2}(u+mw)] \quad (2.11)$$

$$0 = (\frac{\partial^2 w}{\partial y^2} - B\frac{\partial w}{\partial y}\frac{\partial \theta}{\partial y}) + Exp(B\theta)[A_1A_3(S\frac{\partial w}{\partial y} - 2Ru) - A_1A_6\frac{M^2}{1+m^2}(mu-w)] \quad (2.12)$$

$$0 = (A_2 + \frac{4Rd}{3})\frac{\partial^2 \theta}{\partial y^2} + S\,\mathrm{Pr}A_5(\frac{\partial \theta}{\partial y}) - Q\,\mathrm{Pr}(\theta) + Ec\,\mathrm{Pr}\,Exp(-B\theta)[(\frac{\partial u}{\partial y})^2 + (\frac{\partial w}{\partial y})^2] + + Ec\,\mathrm{Pr}\frac{A_6M^2}{1+m^2}(u^2+w^2) \quad (2.13)$$

$$0 = \frac{\partial^2 C}{\partial y^2} + SSc\frac{\partial C}{\partial y} - \gamma C(1+n\delta\theta)Exp(-\frac{E_1}{1+\delta\theta}) + ScSo\frac{\partial^2 \theta}{\partial y^2} \quad (2.14)$$

Where

$G = \frac{\beta_T\, g(T_1-T_0)\,L^3}{\nu^2}$ (Grashof number), $B = m(T_1-T_0)$ (Viscosity parameter)

$M^2 = \frac{\sigma_f \mu_e^2 H_o^2}{L}$ (Magnetic parameter), $Rd = \frac{4\sigma^{\bullet} T_o^3}{\beta_R k_f}$, (Radiation parameter)

$R = \frac{\Omega L}{\nu}, \mathrm{m} = \omega_e\tau_e$ (Rotation parameter), $\mathrm{m} = \omega_e\tau_e$ (Hall parameter),

$Q = \frac{Q_H \nu}{Lk_f}$ (Heat source parameter), $\mathrm{Pr} = \frac{\mu_f C_p}{k_f}$, (Prandtl number),

$Sc = \frac{\nu}{D_B}$ (Schmidt number), $\gamma = \frac{k_c \nu}{L}$ (Chemical reaction parameter),

$Sr = \frac{D_T(T_1 - T_2)}{T_m(C_1 - C_2)}$ (Soret parameter), $\theta_w = \frac{T}{T_2}, \delta = \theta_w - 1,$ (Temperature difference ratio), $\mathrm{E}_1 = \frac{E_a}{KT_2}$ (Activation energy parameter), $A_1 = (1-\varphi)^{2.5}$ $A_2 = \frac{k_{nf}}{k_f},$ $A_3 = 1-\varphi+\varphi(\frac{\rho_s}{\rho_f})$ $A_4 = 1-\varphi+\varphi((\frac{(\rho\beta)_s}{(\rho\beta)_f}), A_5 = 1-\varphi+\varphi\frac{(\rho C_P)_s}{(\rho C_P)_f},$

$A_6 = (1+\frac{3(1-\sigma)\phi}{(\sigma+2)}), \sigma = \frac{\sigma_s}{\sigma_f}$

The boundary conditions (2.5) reduce to

$$u(\pm 1) = 0, \mathrm{w}(\pm 1) = 0, \theta(-1) = 1, \theta(+1) = 0, C(-1) = 1, C(+1) = 0 \qquad (2.15)$$

3. MTHOD OF SOLUTION

The equations (2.11 - 2.14) are highly nonlinear nature and cant resolved exactly. Using Galerkin finite element analysis with quadratic interpolation polynominal the governing equation have been executed to explore the impact of the governing parameters G/M/B/ Rd/Ec/A11/B11/E1δ and γ on velocity, temperature and nanoconcentration.

4. COMPARISON:

In absence ofporous medium (K=0) and Hall effect (m=0) the results are good agreement with Gopi [7].

Parameter		Swcnt-Water nanofluid				Mwcnt-Water nanofluid			
		Gopi [7]		Present Results		Gopi [7]		Present Results	
		Nu(+1)	Sh(+1)	Nu(+1)	Sh(+1)	Nu(+1)	Sh(+1)	Nu(+1)	Sh(+1)
R	0.25	0.498652	0.348847	**0.498655**	**0.348845**	0.497092	0.349132	**0.497096**	**0.349133**
	0.50	0.498651	0.348849	**0.498650**	**0.348852**	0.497092	0.349130	**0.497099**	**0.349132**
	1.00	0.498649	0.348852	**0.498651**	**0.348855**	0.497122	0.349128	**0.497121**	**0.349129**
Rd	0.5	0.498655	0.348846	**0.498657**	**0.348849**	0.497276	0.349135	**0.497263**	**0.349131**
	1.5	0.499252	0.348737	**0.499250**	**0.348739**	0.498381	0.349043	**0.498382**	**0.349049**
	5.0	0.499604	0.348672	**0.499600**	**0.348675**	0.499134	0.348915	**0.499133**	**0.348916**
Ec	0.05	0.498655	0.348846	**0.498652**	**0.348847**	0.497076	0.349135	**0.497079**	**0.349139**
	0.1	0.498673	0.348843	**0.498669**	**0.348845**	0.497144	0.349381	**0.497142**	**0.349388**
	0.12	0.498706	0.348837	**0.498707**	**0.348839**	0.497169	0.349632	**0.497163**	**0.349627**
Q	2	0.499236	0.348742	**0.499238**	**0.348745**	0.498335	0.348907	**0.498339**	**0.348901**
	4	0.498655	0.348846	**0.498657**	**0.348849**	0.497097	0.349396	**0.497100**	**0.349399**
	6	0.498082	0.34895	**0.498088**	**0.34899**	0.495818	0.350121	**0.495827**	**0.350117**
ϕ	0.05	0.498656	0.348846	**0.498655**	**0.348842**	0.497078	0.349138	**0.497067**	**0.349136**
	0.10	0.498601	0.348856	**0.498605**	**0.348855**	0.497004	0.349149	**0.497001**	**0.349155**
	0.12	0.498547	0.348867	**0.498545**	**0.348869**	0.496894	0.349173	**0.496898**	**0.349178**

Parameter		Swcnt-Water nanofluid				Mwcnt-Water nanofluid			
		Gopi [7]		Present Results		Gopi [7]		Present Results	
		Sh(-1)	Sh(+1)	Sh(-1)	Sh(+1)	Sh(-1)	Sh(+1)	Sh(-1)	Sh(+1)
Sr	0.5	0.748156	0.348846	**0.748159**	**0.348841**	0.747505	0.349135	**0.747527**	**0.349121**
	1.0	0.747883	0.348968	**0.747885**	**0.348969**	0.746915	0.349396	**0.746911**	**0.349369**
	1.5	0.747613	0.349093	**0.747604**	**0.349099**	0.746304	0.349669	**0.746313**	**0.349656**
E1	0.1	0.748156	0.348846	**0.748166**	**0.348841**	0.747505	0.349135	**0.747509**	**0.349167**
	0.2	0.727272	0.356813	**0.727274**	**0.356811**	0.726018	0.357372	**0.726023**	**0.357379**
	0.3	0.710376	0.363286	**0.710380**	**0.363293**	0.701005	0.367008	**0.701002**	**0.367011**
δ	0.2	0.748156	0.348846	**0.748155**	**0.348841**	0.747505	0.349135	**0.747503**	**0.349131**
	0.3	0.753602	0.347509	**0.753600**	**0.347511**	0.752358	0.348056	**0.752359**	**0.348072**
	0.4	0.758337	0.346342	**0.758344**	**0.346344**	0.756482	0.347166	**0.756497**	**0.347161**

5. RESULTS AND DISCUSSION:

In this analysis an attempt has been made to investigate the effect of Hall currents, variable viscosity, activation energy on convective heat transfer flow of ethylene based Swcnt and Mwcnt nanofluidsthrough a porous medium in a vertical channel in the presence of heat generating sources. The non-linear, coupled equations have been executed numerically for different variations.The velocity,temperature and nanoconcentrations have been displayed through different graphs.

Figs. 2(a)-2(c) exhibit the effect of Grashof number (G) on flow variables(u, w,θ). It is found from the profiles that increase in G results in an enhancement invelocity components and temperature in both Swcnt and Mwcnt-Eg nanofluids.

Figs.3(a)-3(c) represents u, w, and θ with magnetic parameter(M). Higher the Lorentz force, smaller the velocity components and larger the temperature in the flow region. This force tends to lessen the motion of the fluid for higher values of M, as a consequence the velocity reduces.

The effect of porous medium on flow variables can be seen from figs.4(a)-4(c). Increase in inverse Darcy parameter(K) leads to a depreciation in u and enhancement in w. This is due to the fact that increase in the obstruction of the fluid motion with increase in the inverse Darcy parameter leads to a reduction in u and w. Fig.4(c), the temperature distribution increases with increase in values of K as a result of growth in the thickness of thermal boundary layer owing to Darcy drag developed by the porous medium.

The effect of variable viscosity (B) is exhibited in figs.5(a)-5(c). All the flow variables experience augmentation with rising values of viscosity parameter (B) in both types of nanofluids.This may be due to the fact that increase in B leads to the thickening of the momentum and thermal boundary layers.

The effect of Hall currents(m) on u, $w$and θ is demonstrated in figs.6(a)-6(c).From the profiles we notice that the momentum and thermal boundary layers becomes thicker for higher values of mwhich results in an enhancement velocity components and temperature in the flow region in both types of nanofluids.From the profiles we find that the values of velocity components(u, w) in Eg-Swcnt nanofluid are lesser than those in Eg based Mwcnt nanofluid while opposite behaviour is noticed in the case of temperature distribution.

Figs.7(a)-7(c) indicatethe effect of rotation parameter (R) on u, w and θ. Higher the Coriolis force,smaller the axial velocity,temperature and larger the transverse velocity(w).This indicates that the increase in rotation parameter enhances the growth of the momentum boundary layer and decays the thermal boundary layer thickness in Eg based Swcnt and Mwcnt nanofluids.

Figs.8(a)-8(c) represent the effect of thermal radiation(Rd) on flow variables u, w and θ. With increase in radiation parameter (Rd), the thickness of momentum and thermal boundary layers grow which results in an augmentation in both the velocity components and thermal radiations.This may be due to the fact that increase in Ec leads to growth of the thermal boundary layer in both types of nanofluids.From the profiles we find that the values of velocity components (u, w) in Swcnt-Eg nanofluid are smaller than those in Mwcnt-Egnanofluid. While opposite behaviour is observed in the case of temperature in the flow region.

From figs.9(a)-9(c) we notice a reduction in axial velocity u,enhancement in transverse velocity (w) and temperature (θ) with higher dissipative force (Ec). From the profiles we find that the values of f', g and θ in Swcnt-Eg nanofluid are smaller than those Mwcnt-Eg nanofluid.

Figs.10(a)-10(c) demonstrates the variation of u, $w$and θ with heat source Q. In the presence of heat generating source (Q>0), the axial velocity and the temperature depreciate and transverse velocity(w) upsurges in the flow region.Thus the thickness of thermal boundary layer becomes thinner with increasing values of Heat generating source parameter (Q).From the profiles we find that the values of axial velocity u and temperature in Swcnt -Eg nanofluid are greater than those in Mwcnt-Eg nanofluid. In the case of secondary velocity(w) in Swcnt-Eg nanofluid are lesser than those in Mwcnt-Eg nanofluid for $Q \leq 0.1$ and for higher $Q \geq 0.3$ the values of w in Swcnt-Eg nanofluid are greater than those in Mwcnt-Eg nanofluid.

The effect of nano particle volume fraction (ϕ) on u, w and θ can be seen from figs.11(a)-11(c).The axial velocity and temperature decrease while the transverse velocity (w) augments with rising values of nano particle volume fraction (ϕ).When the volume of the nanoparticle value fraction increases the thermal conductivity grows and hence enhances the momentum boundary layer thickness.This is due to the fact that with increase in ϕ, the thermal boundary layer becomes thinner in the boundary layer.From the graphs we find that the values of u, $w$and θ in Swcnt-Eg nanofluid are relatively greater than those in Mwcnt-Egnanofluid.In the case of secondary velocity (w), its values in Swcnt-Eg nanofluid are relatively smaller than those in Mwcnt-Eg nanofluid.

Figs.12(a)-12(c) depicts the effect of Prandltnumber(Pr) on flow variables.From the profiles we notice that lesser the thermal diffusivity, smaller the axial velocity,temperature and larger the transverse velocity.From the profiles we find that the values of w,θ in Swcnt-Eg nanofluid are relatively greater than those in Mwcnt-Eg nanofluid. In the case of secondary velocity(w) we find that for $Pr \leq 0.62$,the values of w in Swcnt-Eg nanofluid are lesser than those in Mwcnt-Eg nanofluid and for higher $Pr \geq 1.62$,an opposite behaviour is observed in the values of w.

Figs.13(i)-(ii)((a)-13(c)) represents the nanoconcentration (C)with Schmidt number (Sc), Sorret parameter (Sr),chemical reaction parameter (γ). From fig.13(a) we find that lesser the molecular diffusivity,smaller the concentration. Higher the thermo-diffusivity effects larger the concentration in the flow field(fig.13(b)). From 13(c) we notice a depreciation in chemical reaction case (γ>0). The variation of nanoconcentration (C) with different parameters Sc,Sr,γ,E1,δ and n shows that the values of concentration C in Swcnt-Eg nanofluid are relatively greater than those in Mwcnt-Eg nanofluid with variation in Sc,while for variations in Sr,γ and E1 the values of concentration in Swcnt-Eg nanofluid are relatively smaller than those in Mwcnt-Eg nanofluids and for variations in Sc,δ and n, a reverse behaviour is noticed in C.

Figs.13(i)-(ii)(a)-14(c) exhibit the variation of nano concentration (C) with activation energy parameter (E1), temperature difference ratio(δ1) and index number n. From fig.13(a) we notice a growth in nano concentration with higher values of E1. For larger values of δ1 and n, the concentration experiences a depreciation in the flow field.

From the above analysis,we find that the values of the axial velocity in Swcnt-Eg are relatively greater than those in Mwcnt-Eg nanofluid variation in G/Rd/Ec/Q/φ and Pr, while an opposite trend is observed in f' with rising values of M/K/B/m/R

The values of the transverse velocity in Swcnt-Eg are relatively greater than those in Mwcnt with increasing values K/B/m/Rd/Ec/Q/Pr while reversed effect is noticed with increasing values of G/M/R/ϕ. The values of temperature(θ) in Swcnt are always greater than those values in Mwcnt for all parametric variations.

The shear stress components (τx,τz) and rate of heat transfer (Nu) at the walls η=±1 have been presented in table 2 for different parametric variations. It is found that the stress components and Nusselt number augment at both the walls with rising values of Grashof number(G) in Swcnt&Mwcnt nanofluids.Higher the Lorentz force, larger the stress components and smaller the Nusselt number at η=±1 in Swcnt nanofluid while in Mwcnt nanofluid τxreduces,Nu enhances atη=±1. τz enhances atη=-1 and reduces at η=+1. Increase in porous parameter (K) reduces τx,τz at η=±1,Nu reduces at η=-1,τz enhances at η=+1, In Swcnt nanofluid case while in Mwcnt nanofluid case, τx,Nu reduces at η=±1, τz enhances at η=-1 and reduces at η=+1. Both stress components and Nusselt number experiences an enhancement atη=±1 in both Swcnt and Mwcnt nanofluids with higher values of Hall parameter(m). With respect to rotation parameter (R),τx reduces, τz and Nu enhances in Swcnt atη=+1 while in Mwcnt caseτx,Nu decay,τz grows at η=±1 with higher values of R. With rising values of viscosity parameter B,we notice an augmentation in τx,τz and at η=±1 in Swcnt nanofluid case while in Mwcnt nanofluidτx,Nu decays,τy grows at both the walls. In the presence of heat generating source (Q>0), stress components depreciate at η=±1 ,in both Swcnt and Mwcnt nanofluids. The rate of heat transfer upsurges in Swcnt case and decays in Mwcnt case at both the walls. Higher the thermal radiation, larger the stress components at η=±1 in both Swcnt and Mwcnt nanofluids. The Nusselt number reduces in Swcnt nanofluid and enhances in Mwcnt nanofluid at η=±1 with rising values of Rd.

Higher the dissipative energy (Ec), larger τx, smaller Nu atη=±1 in Swcnt case while in caseτy,Nu grows at η=±1 . The stress component τx reduces at η=-1 and enhances at η=+1 in both types of nanofluids. With rising values of nanoparticle volume fraction (φ),τx,τz decay at η=±1 in both types of nanofluids. Nu enhances in Swcnt case and reduces in Mwcnt case at η=±1. With respect to Prandtl number(Pr),τx,τz decay,Nu growsat η=±1 in Swcnt case while in Mwcnt caseτx,τz,Nu decay at η=-1 and η=+1 ,τx,τy growand Nu decays with increase in Ec. From the above analysis we find that the value of stress components at the left wall η=-1 in Swcnt nanofluid are relatively smaller than those in Mwcntnanofluid for all parametric variations.

With higher values of G/K/B/R/Q/Rd/EC/φ/Pr,the values ofτx,τy in Swcnt case are smaller than those in Mwcnt case. For increase in magnetic parameter(M) and Hall parameter (m) values of τx,τy in Swcnt nanofluid are relatively greater than those in Mwcnt nanofluid. The values of the rate of heat transfer at the left wallsη=-1 in Swcntcase are much higher than those in Mwcnt case while at η=+1 an opposite effect is observed in the behaviour of Nu for all parametric variations.

The rate of mass transfer(Sherwood number) at η=±1 are presented in table 3 for different values of Sc,Sr,γ,E1,δ&n. Lesser the molecular diffusivity,larger the Sh at η=-1 and smaller Sh at η=+1,while an opposite trend is noticed in Sh with higher thermos-diffusion effect. The rate of mass transfer atη=-1 increases while at η=+1 decays in the degenerating chemical reaction case. Increase in the activation energy parameter (E1) reduces Sh at η=-1 and enhances Sh at η=+1.For higher values of temperature difference ratio(δ)/index number(n),we notice augmentation in Sh at η=-1 and reduction at η=+1. From the tabular values we find that the Sherwood number at η=-1 in Swcnt nanofluid are much smaller than in Mwcnt nanofluid while a reverse trend is noticed in Sh at η=+1.

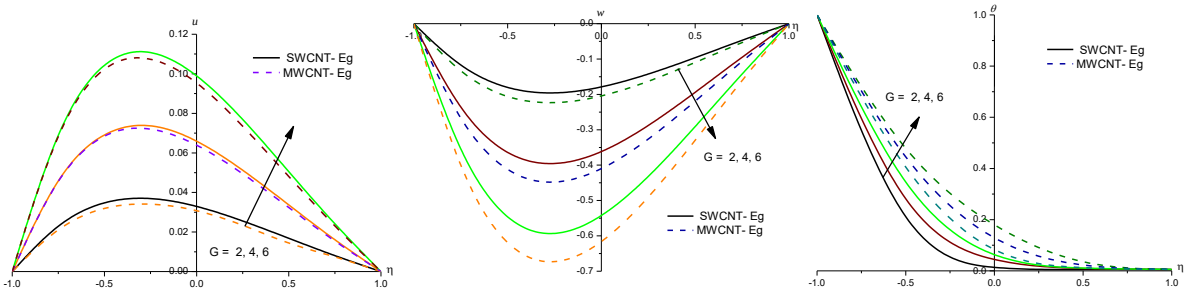

Fig.2 : Variation of [a] Axial velocity (*u*), [b] Secondary velocity(*w*), [c] Temperature(θ), with G
M=1.0, K=0.10, B=0.2, *m*=0.2, R=2, Rd=2, Ec=0.5, Q=0.1, ϕ=0.1, Pr=0.62

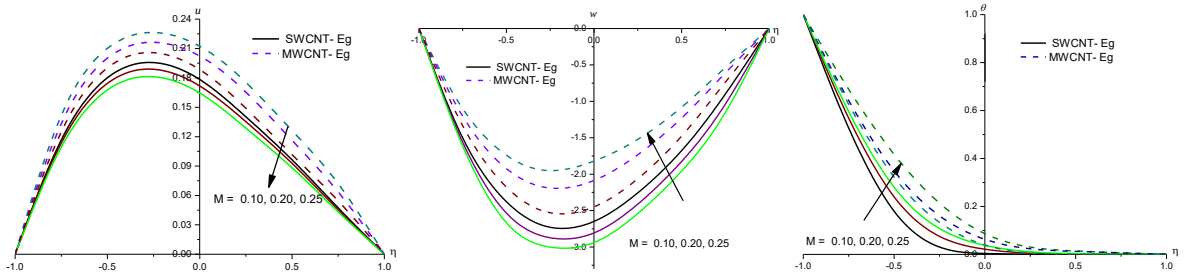

Fig.3 :Variation of [a] Axial velocity (*u*), [b] Secondary velocity(*w*), [c] Temperature(θ), with M
G=2, K=0.10, B=0.2, *m*=0.2, R=2, Rd=2, Ec=0.5, Q=0.1, ϕ=0.1, Pr=0.62

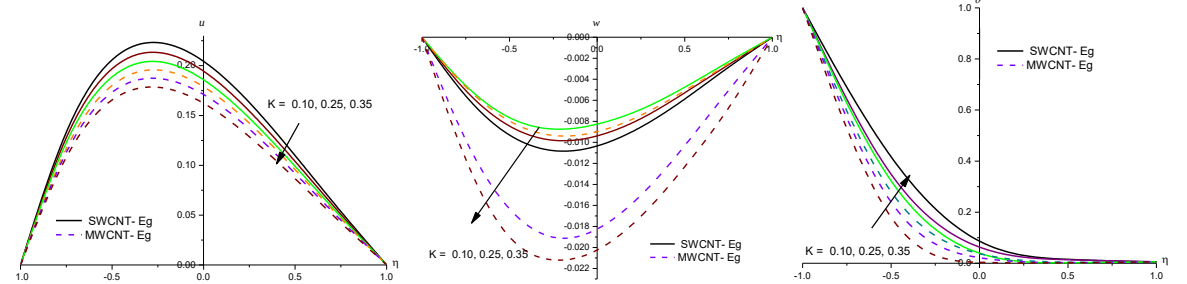

Fig.4 :Variation of [a] Axial velocity (*u*), [b] Secondary velocity(*w*), [c] Temperature(θ), with K
G=2, M=1.0, B=0.2, *m*=0.2, R=2, Rd=2, Ec=0.5, Q=0.1, ϕ=0.1, Pr=0.62

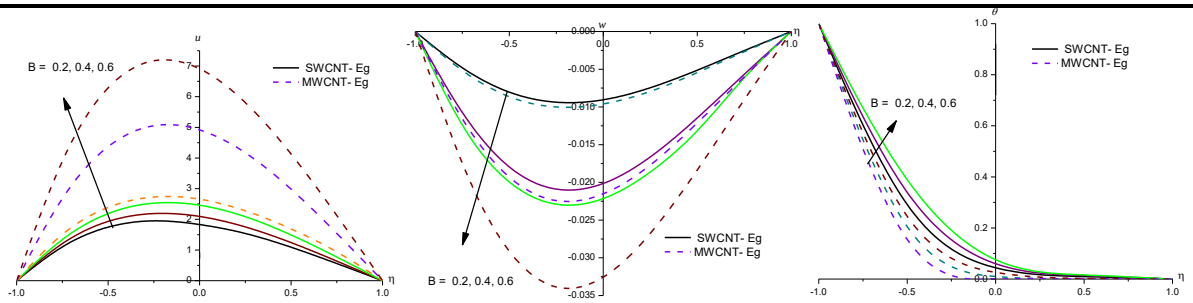

Fig.5 :Variation of [a] Axial velocity (u), [b] Secondary velocity(w), [c] Temperature(θ), with B
G=2, M=1.0, K=0.10, m=0.2, R=2, Rd=2, Ec=0.5, Q=0.1, ϕ=0.1, Pr=0.62

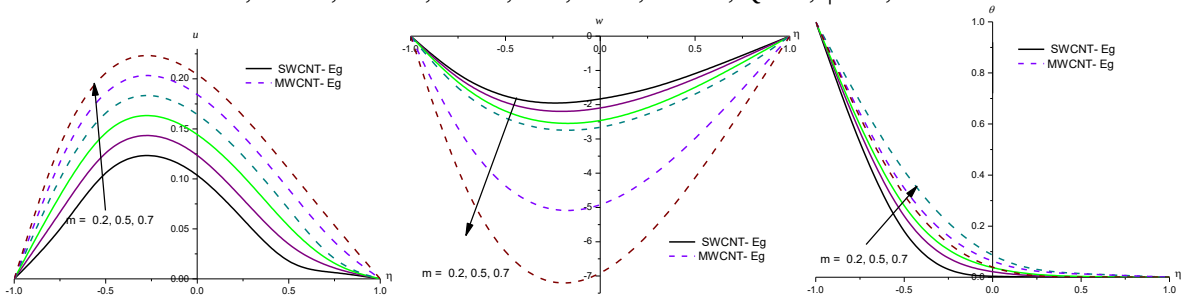

Fig.6 :Variation of [a] Axial velocity (u), [b] Secondary velocity(w), [c] Temperature(θ), with m
G=2, M=1.0, K=0.10, B=0.2, R=2, Rd=2, Ec=0.5, Q=0.1, ϕ=0.1, Pr=0.62

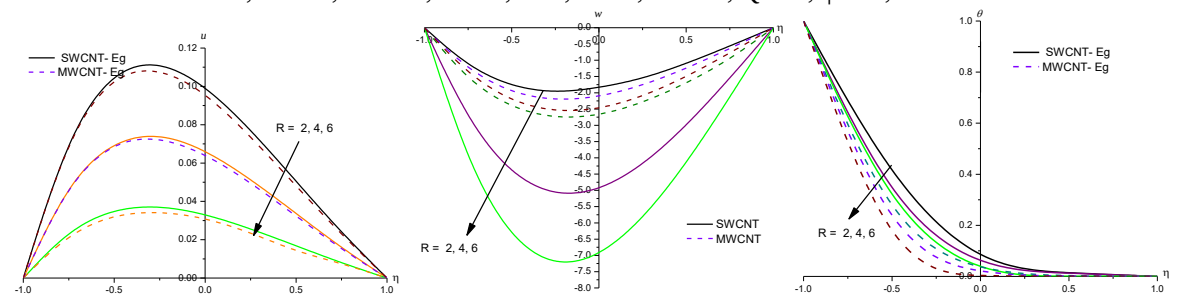

Fig.7 :Variation of [a] Axial velocity (u), [b] Secondary velocity(w), [c] Temperature(θ), with R
G=2, M=1.0, K=0.10, B=0.2, m=0.2, Rd=2, Ec=0.5, Q=0.1, ϕ=0.1, Pr=0.62

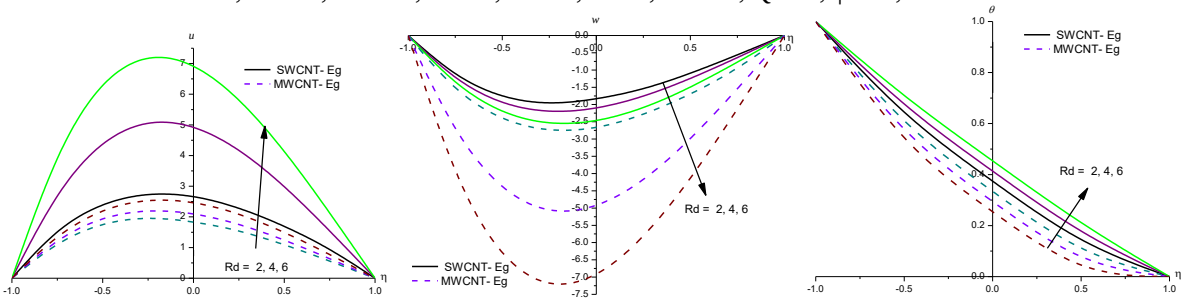

Fig.8 :Variation of [a] Axial velocity (u), [b] Secondary velocity(w), [c] Temperature(θ), with Rd
G=2, M=1.0, K=0.10, B=0.2, m=0.2, R=2, Ec=0.5, Q=0.1, ϕ=0.1, Pr=0.62

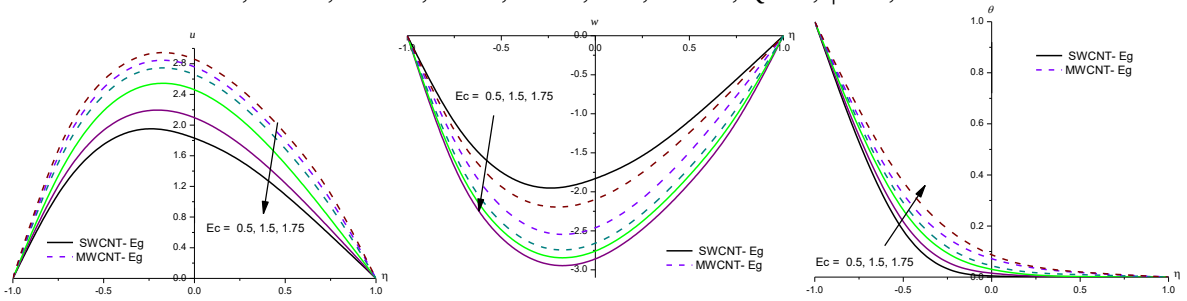

Fig.9 :Variation of [a] Axial velocity (u), [b] Secondary velocity(w), [c] Temperature(θ), with Ec
G=2, M=1.0, K=0.10, B=0.2, m=0.2, R=2, Rd=2, Q=0.1, ϕ=0.1, Pr=0.62

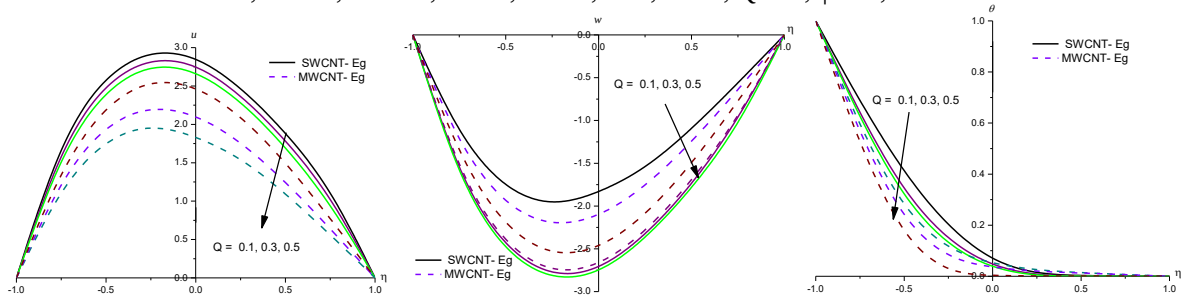

Fig.10 :Variation of [a] Axial velocity (u), [b] Secondary velocity(w), [c] Temperature(θ), with Q
G=2, M=1.0, K=0.10, B=0.2, m=0.2, R=2, Rd=2, Ec=0.5, ϕ=0.1, Pr=0.62

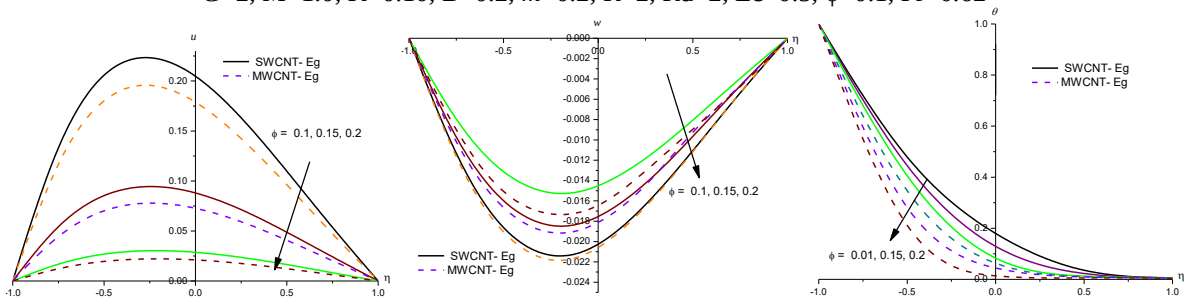

Fig.11 :Variation of [a] Axial velocity (u), [b] Secondary velocity(w), [c] Temperature(θ), with ϕ
G=2, M=1.0, K=0.10, B=0.2, m=0.2, R=2, Rd=2, Ec=0.5, Q=0.1, Pr=0.62

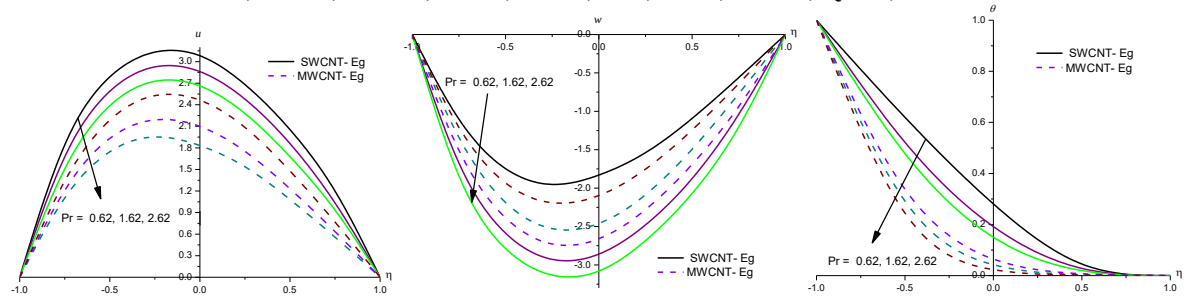

Fig.12 :Variation of [a] Axial velocity (u), [b] Secondary velocity(w), [c] Temperature(θ), with Pr
G=2, M=1.0, K=0.10, B=0.2, m=0.2, R=2, Rd=2, Ec=0.5, Q=0.1, ϕ=0.1

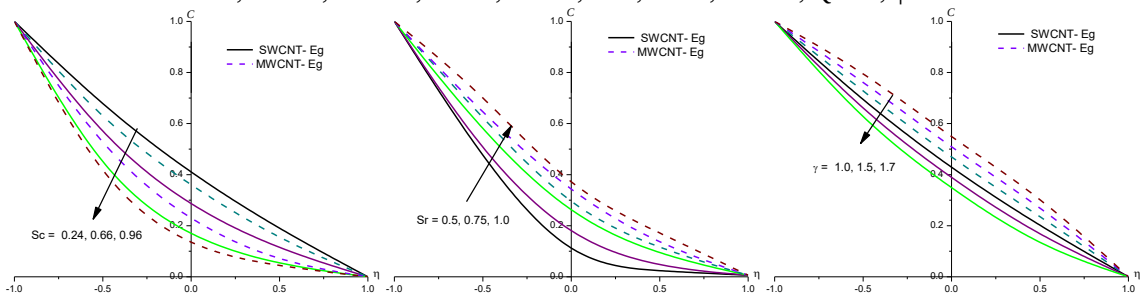

Fig.13(i) : Variation of Nanoconcentration(C) with E1, δ, n

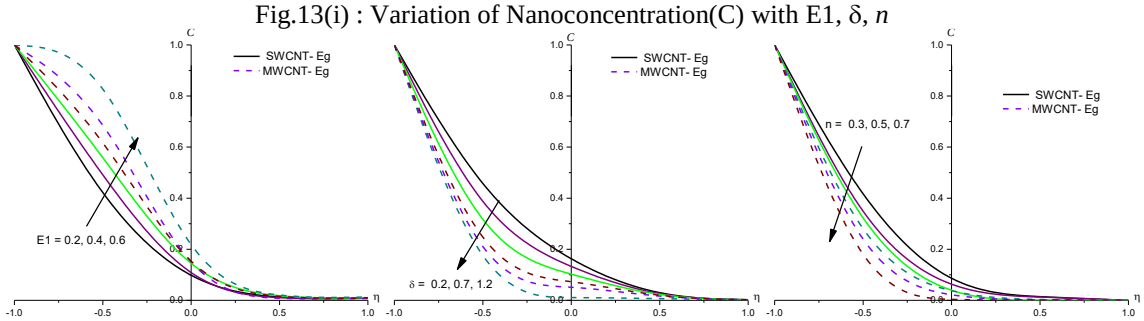

Fig.13(ii) : Variation of Nanoconcentration(C) with Sc, Sr, γ

Table 2 :Shear Stress(τx,τz) and Nusselt number(Nu) with SWCNT-EG & MWCNT-EG on the walls at $\eta = -1$

Parameter		EG-SWCNT			EG-MWCNT		
		τx(-1)	τz(-1)	Nu(-1)	τx(-1)	τz(-1)	Nu(-1)
G	0.2	0.13833	-0.0056748	0.501032	0.139516	-0.0058577	0.502264
	0.4	0.27665	-0.0117252	0.501042	0.279032	-0.0117156	0.502267
	0.6	0.41498	-0.0175878	0.501132	0.418548	-0.0175734	0.502269
M	0.10	1.33914	-0.0301075	0.501031	1.440054	-0.0342246	0.502263
	0.20	1.35355	-0.0397172	0.501027	1.424544	-0.0422908	0.502266
	0.25	1.38328	-0.0586263	0.501022	1.395165	-0.0585782	0.502288
m	0.2	1.10033	-0.4524364	0.501033	1.133135	-0.4840233	0.502261
	0.5	0.78185	-0.5128166	0.501031	0.320932	-0.5459234	0.502253
	0.7	0.61469	-0.5695869	0.501027	0.647827	-0.5919594	0.502264
K	0.10	1.49484	-0.0698632	0.501028	1.49461	-0.0716344	0.502257
	0.25	1.43612	-0.0649837	0.501029	1.44259	-0.0645927	0.502253
	0.35	1.38328	-0.0586263	0.501032	1.39516	-0.0585782	0.502258
B	0.2	1.38395	-0.0567745	0.500088	1.39636	-0.0586535	0.500189
	0.4	1.38382	-0.0586599	0.500107	1.39633	-0.0586526	0.500095
	0.6	1.38381	-0.0587592	0.500126	1.39622	-0.0586505	0.500273
R	2	1.38339	-0.0567461	0.501029	1.39536	-0.0585782	0.502258
	4	1.37261	-0.1186266	0.501032	1.39544	-0.0585782	0.502248

	6	1.38328	-0.1586263	0.501043	1.39516	-0.0585782	0.502258
Q	0.1	1.38373	-0.0557615	0.500468	1.39589	-0.0586241	0.501027
	0.3	1.38375	-0.0586546	0.500271	1.39614	-0.0586402	0.500595
	0.5	1.38378	-0.0586276	0.500191	1.39625	-0.0586468	0.500418
Rd	2	1.38339	-0.0567461	0.501029	1.39516	-0.0585782	0.502258
	4	1.37262	-0.1186266	0.501023	1.39519	-0.0585788	0.502245
	6	1.38329	-0.1586266	0.501021	1.39522	-0.0585789	0.502232
Ec	0.5	1.38339	-0.0567461	0.501029	1.39516	-0.0585782	0.502258
	1.5	1.21642	-0.0483892	0.501035	1.28027	-0.0510397	0.502268
	1.7	1.05968	-0.0394935	0.501044	1.16149	-0.0439422	0.502277
ϕ	0.05	1.38395	-0.0567748	0.500103	1.39636	-0.0586534	0.500226
	0.15	1.38373	-0.0586547	0.500269	1.39615	-0.0586404	0.500579
	0.20	1.38364	-0.0587485	0.500435	1.39593	-0.0586268	0.500955
Pr	0.62	1.38395	-0.0567748	0.500103	1.39636	-0.0586534	0.500226
	1.62	1.38373	-0.0586547	0.500269	1.39615	-0.0586404	0.500359
	2.62	1.38364	-0.0585485	0.500435	1.39593	-0.0586268	0.500955

Table 3 :Shear Stress(τx,τz) and Nusselt number(Nu) with SWCNT-EG & MWCNT-EG on the walls at η = +1

Parameter		**EG-SWCNT**			**EG-MWCNT**		
		τx(+1)	**τz(+1)**	**Nu(+1)**	**τx(+1)**	**τz(+1)**	**Nu(+1)**
G	0.2	0.138339	-0.0056748	0.501032	0.139516	-0.00585778	0.502264
	0.4	0.27665	-0.0117252	0.501032	0.279032	-0.0117156	0.502264
	0.6	0.41498	-0.0175878	0.501032	0.418548	-0.0175734	0.502264
M	0.10	1.33914	-0.0301075	0.501031	1.44005	-0.0342246	0.502263
	0.20	1.35355	-0.0397172	0.50103	1.42454	-0.0422908	0.50226
	0.25	1.38328	-0.0586263	0.501029	1.39516	-0.0585782	0.502258
m	0.2	1.10033	-0.4524344	0.50103	1.13313	-0.48402	0.502261
	0.5	0.78185	-0.5128164	0.501031	0.820932	-0.545924	0.502263
	0.7	0.61469	-0.4695844	0.501032	0.647827	-0.501959	0.502264
K	0.10	1.49484	-0.0698632	0.501028	1.49461	-0.0716344	0.502257
	0.25	1.43612	-0.0649837	0.501029	1.44259	-0.0645927	0.502257
	0.35	1.38328	-0.0586263	0.501029	1.39516	-0.0585782	0.502258
B	0.2	1.38395	-0.0567745	0.500088	1.39636	-0.0586535	0.500189
	0.4	1.38382	-0.0586599	0.500107	1.39633	-0.058652	0.500231
	0.6	1.38381	-0.0586592	0.500126	1.39631	-0.0586505	0.500273
R	2	1.38339	-0.0567414	0.501029	1.39516	-0.0585782	0.502258
	4	1.37261	-0.1186264	0.501029	1.39516	-0.0585782	0.502258
	6	1.38328	-0.0586263	0.501029	1.39516	-0.0585782	0.502258
Q	0.1	1.38373	-0.0567615	0.500468	1.39589	-0.0586241	0.501027
	0.3	1.38373	-0.0586546	0.500271	1.39614	-0.0586402	0.500595
	0.5	1.38378	-0.0586576	0.500191	1.39625	-0.0586468	0.500418
Rd	2	1.38339	-0.0567414	0.501029	1.39516	-0.0585782	0.502258
	4	1.37262	-0.1186264	0.501023	1.39517	-0.0585788	0.502245
	6	1.38329	-0.0586266	0.501021	1.39518	-0.0585789	0.502242
Ec	0.5	1.38339	-0.0567414	0.501029	1.39516	-0.0585782	0.502258
	1.5	1.21642	-0.0483892	0.501035	1.28027	-0.0510397	0.502268
	1.75	1.05968	-0.0394935	0.50104	1.16149	-0.0439422	0.502277
ϕ	0.1	1.38395	-0.0567748	0.500103	1.39636	-0.058654	0.500226
	0.15	1.38373	-0.0586547	0.500269	1.39615	-0.0586404	0.50059
	0.2	1.38364	-0.0586485	0.500435	1.39593	-0.0586268	0.500955
Pr	0.62	1.38395	-0.0567748	0.500103	1.39636	-0.058654	0.500226
	1.62	1.38373	-0.0586547	0.500269	1.39615	-0.0586404	0.50059
	2.62	1.38364	-0.0586485	0.500435	1.39593	-0.0586268	0.500955

able 4 :Shewood number (Sh)with SWCNT-EG & MWCNT-EG on the walls at η = ±1

Parameter		**EG-SWCNT**		**EG-MWCNT**	
		Sh(-1)	**Sh(+1)**	**Sh(-1)**	**Sh(+1)**
Sc	0.25	0.771065	0.337335	0.770768	0.337464
	0.66	1.24332	0.166168	1.24251	0.166416
	0.96	1.57684	0.0990546	1.57567	0.0993372
Sr	0.5	0.748592	0.348651	0.748455	0.348712
	0.75	0.748535	0.348676	0.74833	0.348767
	1.0	0.748479	0.348701	0.748206	0.348822
γ	1.0	0.748479	0.348701	0.748206	0.348822

	1.5	0.809158	0.327131	0.808891	0.327247
	1.7	0.832659	0.319016	0.832395	0.31913
E1	0.2	0.738104	0.352653	0.73783	0.352775
	0.4	0.719661	0.359704	0.719384	0.359828
	0.6	0.703947	0.365731	0.703668	0.365855
δ	0.2	0.748479	0.348701	0.748206	0.348822
	0.7	0.760513	0.345739	0.760238	0.345861
	1.2	0.77168	0.342987	0.771402	0.34311
n	0.3	0.75032	0.348259	0.750047	0.34838
	0.5	0.753997	0.347378	0.753723	0.347499
	0.7	0.757667	0.346500	0.757392	0.346621

6.CONCLUSIONS:

The effect of activation energy,variable viscosity,Hall effects on convective heat and mass transfer flow of Eg based Swcnt and Mwcnt nanofluids have been investigated by solving the governing equations by Finite element method.The findings of this analysis are : Increase in Grashof number(G)/Eckert number(Ec)results in an enhancement invelocity components and temperature in both Swcnt and Mwcnt nanofluids.

1) Higher the Lorentz force(M)/porous permeability(K), smaller the velocity components and larger the temperature in the flow region.
2) All the flow variables experience augmentation with rising values of Hall parametrer (m)/viscosity parameter (B)/radiation(Rd) in both types of nanofluids.
3) The axial velocity and temperature decrease while the transverse velocity (*w*) augments with rising values of nano particle volume fraction (ϕ)/Heat source (Q)/rotation(R).
4) The nanoconcentration (C) reduces with Sc,Chemical reaction parameter (γ)/ temperature difference ratio(δ) and enhances with Soretparameter (Sr)/activation energy parameter(E1).
5) τx reduces,τz and Nu enhance in Swcnt atη=+1 while in Mwcnt caseτx,Nu decay,τz grows at η=±1 with higher values of R.
6) With rising values of viscosity parameter(B),τx,τzgrow at η=±1 in Swcnt nanofluid case while in Mwcnt nanofluid,τx,Nu decay,τz grows at both the walls.
7) Higher the thermal radiation, larger the stress components at η=±1 in both Swcnt and Mwcnt nanofluids.Higher the dissipative energy (Ec), larger τx, smaller Nu atη=±1 in Swcnt case while in Mwcnt caseτy,Nu grows at η=±1.
8) With rising values of nanoparticle volume fraction (φ),τx,τz decay at η=±1 in both types of nanofluids. Nu enhances in Swcnt case and reduces in Mwcnt case at η=±1
9) Higher thermo-diffusion effects,smaller Sh at η=-1 and larger at η=+1. The rate of mass transfer atη=-1 increases while at η=+1,it decays in the degenerating chemical reaction case.
10) Increase in the activation energy parameter (E1) reduces Sh at η=-1 and enhances Sh at η=+1.For higher values of temperature difference ratio(δ)/index number(n), Shupsurges at η=-1 and reduces at η=+1.

7. REFERENCES

[1]. Anuar N., Bachok N., and Pop I., "A stability analysis of solutions in boundary layer flow and heat transfer of carbon nanotubes over a moving plate with slip effect," *Energies*, vol. 11, no. 12, (2018),p. 3243.

[2]. Arundhati V., Sekhar K.V.C., Prasada Rao D.R.V. and Sreedevi G., "Thermal Radiation and Thermo-diffusion effect on Convective Heat and Mass Transfer Flow of a Rotating Nanofluid in a Vertical Channel", *International Conference on Numerical Heat Transfer & Fluid Flow* (NHTFF18), National Institute of Technology (NIT) Warangal, TS, India on Jan 19-21, (2018); Numerical Heat Transfer and Fluid Flow: Select Proceedings of NHTFF 2018 (Springer) pp.73-81. https://DOI.org/10.1007/978-981-13-1903-7_10.

[3]. Barletta, A, Celli, M and Magtyari, E and Zanchini, E: Buoyany MHD flows in a vertical channel the levitation regime Heat and Mass Transfer, V.44, (2007) pp.1005-1013.

[4]. Berrehal H. and Maougal A., "Entropy generation analysis for multi-walled carbon nanotube (MWCNT) suspended nanofluid flow over wedge with thermal radiation and convective boundary condition," *Journal of Mechanical Science and Technology*, vol. 33, no. 1, (2019) pp. 459–464.

[5]. Datta, N anfd Jana, R.N: Effect of wall conductance on hydromagnetic convection of a radiation gas in a vertical channel, Int.J.Heat Mass Transfer, V.19, (1974) pp.1015-1019.

[6]. Dhlamini M., Kameswaran P. K., Sibanda P., Motsa S., and Mondal H., *J. Comp. Design Eng*. 6, (2019)149.

[7]. Gopi P: Effect of heat generating sources on hydromagnetic convective heat transfer flow of rotating swcnt and mwcnt nanofluid in vertical channel with inconstant viscosity, Journal Of Engineering, Computing & Architecture, Volume 14, Issue 01, pp.76-93, JANUARY – 2024, ISSN NO:1934-7197, http://www.journaleca.com/

[8]. Gupta, P.S and Gupta, A.S: Radiation effect on hydromagnetic convection in a vertical channel. Int. J. heat Mass Transfer, V.17, (1973)pp. 1437-1442.

[9]. Kiran Kumar G, Srinivas G, Suresh Babu B, Srikanth GVPN : effects of variable viscosity and thermal conductivity on Mhd convective heat transfer of immiscible fluids in a vertical channel, *International Journal of Engineering Sciences & Research Technology (IJESRT)*, 7(5): (May, 2018), http: // www.ijesrt.com

[10]. Maleque K.A., ,*ISRN Thermo*., V.9, (2013).

[11]. Naganthran K., Nazar R., and Pop I., "Effects of heat generation/absorption in the Jeffery fluid past a permeable stretching/shrinking disc," *Journal of the Brazilian Society of Mechanical Sciences and Engineering*, vol. 41, (2019)pp. 1–12.

[12]. Netai Roy and Dulal Pal : Influence of Activation Energy and Nonlinear Thermal Radiation with Ohmic Dissipation on hydromagnetic convective heat and mass transfer flow of a Casson Nanofluid over Stretching Sheet, Journal of Nanofluids, Vol. 11, No. 6, pp. 819–832, (2022), doi:10.1166/ jon.2022.1882, www.aspbs.com/jon

[13]. Shafiq A., Khan I., Rasool G., Sherif E. M., and Sheikh A. H., "Influence of single- and multi-wall carbon nanotubes on magnetohydrodynamic stagnation point nanofluid flow over variable thicker surface with concave and convex effects," *Mathematics*, vol. 8, no. 104, (2020).

[14]. Shamshuddin M. D., Animasaun Isaac Lare, Olakunle Salawu Sulyman& Pudi Srinivasa Rao : Dynamics of ethylene glycol conveying MWCNTs and ethylene glycol conveying SWCNTs: Significant joule heating and thermal radiation, Numerical Heat Transfer, Part A: International Journal of Computation and Methodology, 2023, https://www.tandfonline.com/ loi/unht20, https://doi.org/10.1080/10407782. 2023. 2195130

[15]. Shamshuddin MD., Salawu S.O., Kanayo Kenneth Asogwa, Srinivasa Rao P.: Thermal exploration of convective transportation of ethylene glycol based magnetized nanofluid flow in porous cylindrical annulus utilizing MOS2 and Fe3O4 nanoparticles with inconstant viscosity, Journal of Magnetism and Magnetic Materials 573 (2023) 170663, https://doi.org/10.1016/j.jmmm.2023.170663

[16]. Sreedevi G. and Prasada Rao D.R.V. "Effect of Dissipation and Radiation on Convective Heat Transfer Flow of a Rotating Cu-Water Nano-fluid in a Vertical Channel", International Journal for Research and Development in Technology (IJRDT), Vol. 8(2) (2017) pp. 21-30.

[17]. Srinivasa Rao P, ShamshuddinMD. : Second-order slip and Newtonian cooling Impact on unsteady mixed convective radiative chemically reacting fluid with Hall current and cross-diffusion over a stretching sheet, Heat Transfer. 2021;1–26., wileyonlinelibrary. com/ journal/htj, DOI: 10.1002/htj.22234

[18]. Sulochana C and Ramakrishna G.N. : Effect dissipation, thermal radiation. Radiation absorbtion on convective heat and mass transfer flow in a non-uniformly heated vertical channel, Adv.in Phy.Theories and Applications, Vol.No.44, (2015) pp.78-91 ISSN 2225-0638, www.iiste.org

[19]. Suvarna T : Finite element appoach of hydromagnetic heat and mass transfer flow of rotating fluid in a channel with activation energy: Presented in *International Conference On Innovations And Developments In Mathematical Sciences, And Technology* (ICIDMST-2023), June 29th – 31st, 2023, Sri Krishnadevaraya University, A.P., India

[20]. Vijayalakshmi P.: Effect of Thermal Radiation on Non-Darcy Hydromagnetic Convective Heat and Mass Transfer Flow of a Water-SWCNT's Nanofluid in a Cylindrical Annulus with Thermo-Diffusion and Chemical Reaction, Journal of Xi'an University of Architecture & Technology, Volume XIII, Issue 3, 2021, PP.16-29, ISSN No : 1006-7930.